Supplementary Information

Glucose Oxidation over Ultrathin Carbon-coated Perovskite Modified TiO_2 Nanotube Photonic Crystals with High-efficiency Electron Generation and Transfer for Photoelectrocatalytic Hydrogen Production

Yajun Zhang, Bo Tang, Zhongyi Wu, Huijie Shi, Yanan Zhang, Guohua Zhao*

Department of Chemistry, Shanghai Key Lab of Chemical Assessment and Sustainability, Tongji University, Shanghai 200092, People's Republic of China.

*Corresponding Author: Phone: +(86)-21-65981180. Fax:+(86)-21-65982287

E-mail: g.zhao@tongji.edu.cn

Experiment Section

Preparation of C@Cr-$SrTiO_3$/TiO_2 NTPC heterostructrues photoanode

TiO_2 NTPC were prepared by a three-step electrochemical anodic oxidation procedure according to the literature.[1, 2] The deposition of Cr-droped $SrTiO_3$ (Cr-$SrTiO_3$) onto TiO_2 NTPC substrate electrode was achieved using the hydrothermal process.[3] And then, an aqueous solution of glucose as carbon precursor at various concentrations (1 mg mL^{-1}, 2 mg mL^{-1}, 3mg mL^{-1} and 4 mg mL^{-1}). The Cr-$SrTiO_3$/TiO_2 NTPC photoanodes were immersed in the above glucose solution for 15 min. After the as-photoanode Cr-$SrTiO_3$/TiO_2 NTPC was annealed at 550 °C under the Nitrogen atmosphere for 2 h to produce the ultrathin carbon layers-coated Cr-$SrTiO_3$/TiO_2 NTPC (C@Cr-$SrTiO_3$/TiO_2 NTPC) photoanode.

Characterization methods

The chemical compositions of the as-prepared sample was determined by X-ray photoelectron spectroscopy (XPS, AXIS Ultra HSA, Kratos Analytical Ltd., UK) under ultrahigh vacuum (< 10^{-8} torr) using a monochromatic Al Kα X-ray source operating at 150 W. The survey and high-resolution spectra were collected at fixed analyzer pass energies of 160 and 20 eV, respectively. Samples were mounted in floating mode in order to avoid differential charging. Binding energies were referenced to the C 1s binding energy of adventitious carbon contamination which was set at 284.6 eV. The UV-vis diffuse reflectance absorption spectra (UV-vis DRS) were recorded by Avalight-DHS UV-Vis absorbance measurement (Avantes, Netherlands).The morphologies of sample were observed by field emission scanning electron microscope (FESEM, Hitach S-4800, Japan). Detailed microstructural features of the sample electrodes were investigated by transmission electron microscopy (TEM, JEM2100, JEOL, Japan), using a JEM-2000EX electron microscope operated at 200 kV. Selected area electron diffraction (SAED) and HR-TEM were applied to identify the crystal structure and to investigate the atomic scale microstructure of sample electrodes, respectively. The crystalline phase of the samples were analyzed by X-ray diffraction (XRD, D8 Focus X-ray diffractometer, Bruker, Germany), using Cu Kα radiation (λ =

1.540598 Å). Raman spectra were obtained on a Renishaw inVia Raman Microscope using a 50 × long working distance objective to focus the laser beam at λ = 514 nm. A silicon wafer was used to calibrate the spectrometer at a Raman band of 520 ± 0.5 cm^{-1}.

Photoelectrochemical measurements and PEC hydrogen production

The photoelectrochemical measurements were carried out in a three-electrode one-compartment photoelectrochemical cell with a quartz window to facilitate irradiation of as-prepared photoanode surface. The sample photoelectrode, a saturated calomel electrode (SCE) and a Pt foil were served as the working electrode, reference electrode and counter electrode, respectively. And 0.5 mol L^{-1} KOH (pH = 13.7) with or without glucose solution as electrolyte solution. The detail photocurrent response and open circuit photovoltage of as-prepared photoanodes materials were measured under a chopped irradiation from 300 W Xe high-pressure short-arc xenon lamp (PLS-SXE300, PerfectLight Technology Co, Ltd., Beijing). The intensity of the light source was calibrated with a Si diode (Newport) to visible light irradiation (wavelength of 420-800 nm, light intensity of 100 mW cm^{-2}).

All the electrochemical measurements were performed on an electrochemical workstation (CHI 660D) at the room temperature. The scan rate is fixed at 100 mV s^{-1} for all the linear sweep voltammetry (LSVs) of as-prepared sample photoanode investigated. The forward scans swept the potential window from negative to positive. The photoelectrochemical stability of sample electrode was evaluated by measuring the photocurrent densities produced under chopped visible light irradiation (light on or off: 50 s) at the fixed electrode potential of 0.6 (vs. SCE). Electrochemical impedance spectroscopy (EIS) was performed in dark and under the visible light irradiation at open voltage over a frequency range from 10^5 to 10^{-1} Hz at an overpotential of 10 mV.

The PEC hydrogen production from glucose oxidation was investigated in a gas-closed circulation system (PerfectLight Technology Co, Ltd., Beijing) equipped with a home-made three-electrode photoelectrochemical dual compartment photoreactor and a volumetric device with a vacuum line. In order to reduce or avoid the influence of the production generated on the photoanode and cathode surface, a glass frit membrane was

used as the electrolyte separator between anode and cathode. The volume of the electrolyte was 100 mL consisting of 0.5 mol L^{-1} KOH with /without 0.1 mol L^{-1} glucose, and as-prepared sample electrode and SCE were used as the photoanode and reference electrode, respectively. Before the measurement, the PEC dual cell was purged with N_2 for 30 min to remove dissolved oxygen in the electrolyte solution. The amount of gas generated in the Pt sheet cathode at -0.3 V (*vs.* SCE) was collected and detected by an online gas chromatography (GC) with a thermal conductivity detector.

1) The photo-to-current conversion efficiency (η, PCE) could be calculated from the current-potentiometry data using the following equation[4, 5]:

$$\eta(\%) = \frac{j_p \times (E_{rev} - |E_{app}|)}{I_0} \times 100 \qquad (1)$$

Where j_p (mA·cm^{-2}) is the photocurrent density, $j_p \times E_{rev}$ is the total power output, $j_p \times |E_{app}|$ is the electrical power input, I_0 (mW·cm^{-2}) is the power density of the incident light, E_{rev} is the standard reversible potential (1.23 V for the water splitting reaction at pH = 0) and $|E_{app}|$ is the absolute value of the applied potential (which is obtained as $E_{app}=E_{means} - E_{ocp}$, where E_{means} is the electrode potential of the electrode potential of the working electrode when j_p is measured under irradiation, and E_{ocp} is the applied potential at the open circuit under the same conditions.

2) The open circuit photovoltage decay (OCPD) rate is closely related to the photoelectron lifetime by the following equation[4, 6]:

$$\tau = (k_B T/e)(dE_{OCV}/dt)^{-1} \qquad (2)$$

where τ is the potential-dependent photoelectron lifetime, k_B is Boltzmann's constant, T is the temperature, e is the charge of a single electron, and dE_{OCV} is the open-circuit voltage at time t.

3) Total Organic carbon (TOC) and Inorganic carbon (IC) were measured with total organic carbon analyzer (multi N/C 3100 TOC/TN analyzer, Analytikjena, Germany), one milliliter of the solution close to the photoanodes after the 6 h reaction was diluted to 50 ml with DI water before the analysis. [2, 7] The TOC was calculated from eqn (3):

$$TOC = TC - IC \qquad (3)$$

Where the TC is total carbon and IC is inorganic carbon. The generated CO_2 would dissolve into the base solution and form carbonate (CO_3^{2-} or HCO_3^{-}) even if after the dilution which the pH was 10.0 measured by pH meter (Shanghai Precision & Scientific Instrument Co. Ltd.,), and then IC would contain the generated CO_2 and absorption of CO_2. As the IC of blank sample only can come from the absorption of CO_2 in air, the

generated CO_2 of each sample should be calculated from Eq(4):

$$\omega_{CO2} = IC - IC_{blank} \quad (4)$$

After the reaction, the carbon of the initial carbon became TOC still in the solution, CO_2 transferring to carbonate and CO escaping into air. Then, we also can get the amount of the generated CO from Eq (5):

$$\omega_{CO} = TOC_{blank} - TOC - \omega_{CO2} \quad (5)$$

Furthermore, the efficiency of the glucose oxidation can be calculated by eqn (6):

$$\eta = [\omega(CO_2) + \omega(CO)] \times 100\% / \omega(C_6H_{12}O_6) \quad (6)$$

1. M. Ye, J. Gong, Y. Lai, C. Lin and Z. Lin, *J Am Chem Soc*, 2012, **134**, 15720-15723.
2. Y. J. Zhang, G. H. Zhao, H. J. Shi, Y. N. Zhang, W. N. Huang, X. F. Huang and Z. Y. Wu, *Electrochimica Acta*, 2015, **174**, 93-101.
3. Z. Jiao, Y. Zhang, T. Chen, Q. Dong, G. Lu and Y. Bi, *Chemistry*, 2014, **20**, 2654-2662.
4. M. Zhong, T. Hisatomi, Y. Kuang, J. Zhao, M. Liu, A. Iwase, Q. Jia, H. Nishiyama, T. Minegishi, M. Nakabayashi, N. Shibata, R. Niishiro, C. Katayama, H. Shibano, M. Katayama, A. Kudo, T. Yamada and K. Domen, *J Am Chem Soc*, 2015, **137**, 5053-5060.
5. Y. Zhang, G. Zhao, Y. Zhang and X. Huang, *Green Chemistry*, 2014, **16**, 3860.
6. F. X. Xiao, J. Miao, H. Y. Wang, H. Yang, J. Chen and B. Liu, *Nanoscale*, 2014, **6**, 6727-6737.
7. S. L. Xie, T. Zhai, W. Li, M. H. Yu, C. L. Liang, J. Y. Gan, X. H. Lu and Y. X. Tong, *Green Chemistry*, 2013, **15**, 2434-2440.

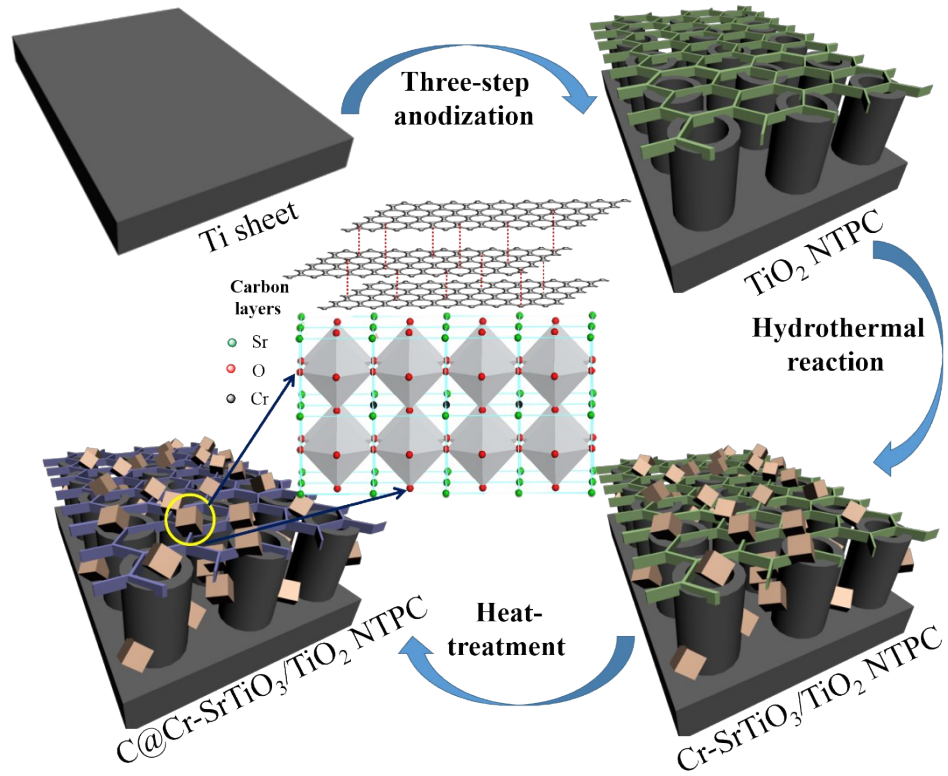

SI-Scheme 1 Schematic illustration of the preparation of the C@Cr-$SrTiO_3$/TiO_2 NTPC heterostructure photoanode

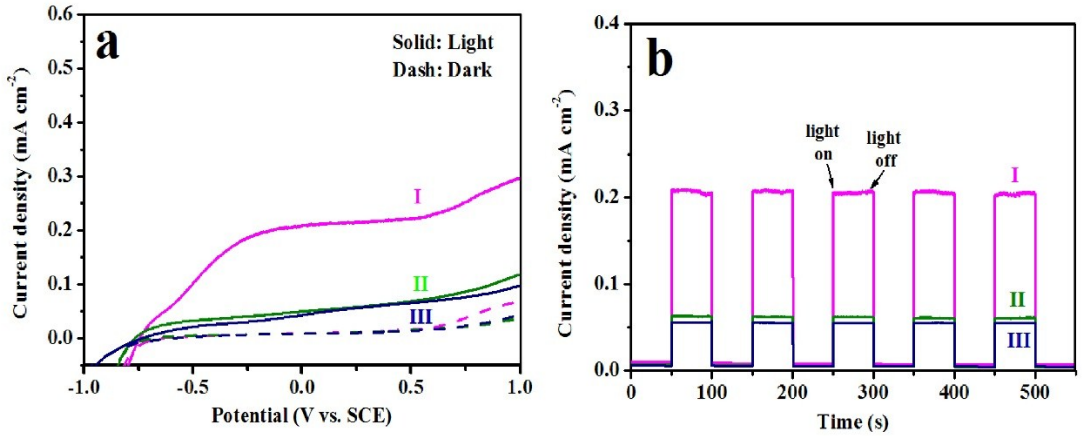

SI-Fig.1 The photoelectrochemical performance of as-prepared photoanode material in various concentration of glucose solution. (a) LSVs in 0.5 mol L^{-1} KOH solution at the scan rate of 100 mV s^{-1} at a potential of -1.0 V to 1.0 V vs. SCE; (b) Chronoamperometric i-t curves in 0.5 mol L^{-1} KOH solution at the bias potential of 0.6 V vs. SCE with chopped visible light irradiation. (I:1mg mL^{-1}; II:3 mg mL^{-1}; III: 4 mg mL^{-1})

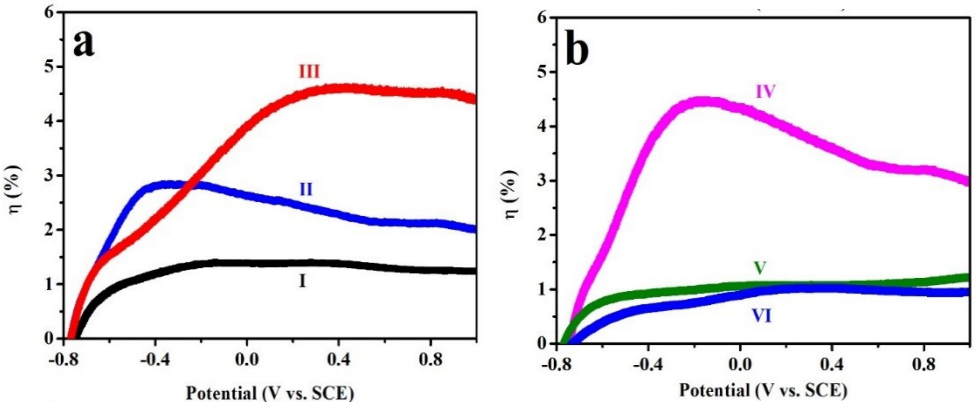

SI-Fig.2 Photoconversion efficiency as a function of applied potential of different photoelectrodes in the various concentration of glucose solution. (a): I: pure TiO_2 NTPC, II Cr-$SrTiO_3$/TiO_2 NTPC, III: C@Cr-$SrTiO_3$/TiO_2 NTPC (2 mg mL^{-1}), (b):IV: C@Cr-$SrTiO_3$/TiO_2 NTPC (1 mg mL^{-1}), V: C@Cr-$SrTiO_3$/TiO_2 NTPC (3 mg mL^{-1}), VI: C@Cr-$SrTiO_3$/TiO_2 NTPC (4 mg mL^{-1})

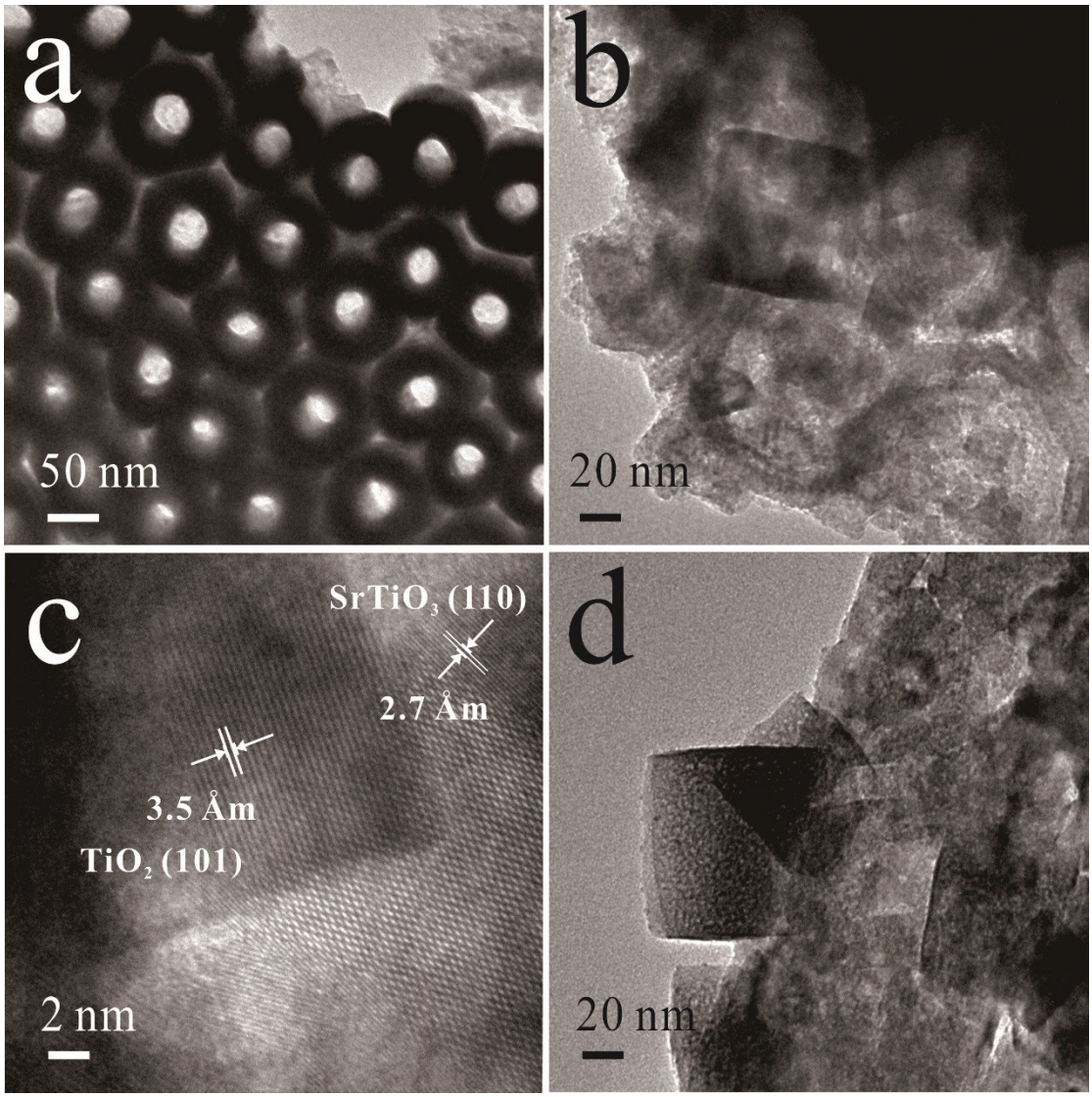

SI-Fig.3 Top view TEM image of TiO_2 NTPC (a) and Cr-$SrTiO_3$/TiO_2 NTPC (b). HR-TEM image of Cr-$SrTiO_3$/TiO_2 NTPC (c). And cross-sectional TEM image of C@ Cr-$SrTiO_3$/TiO_2 NTPC (d).

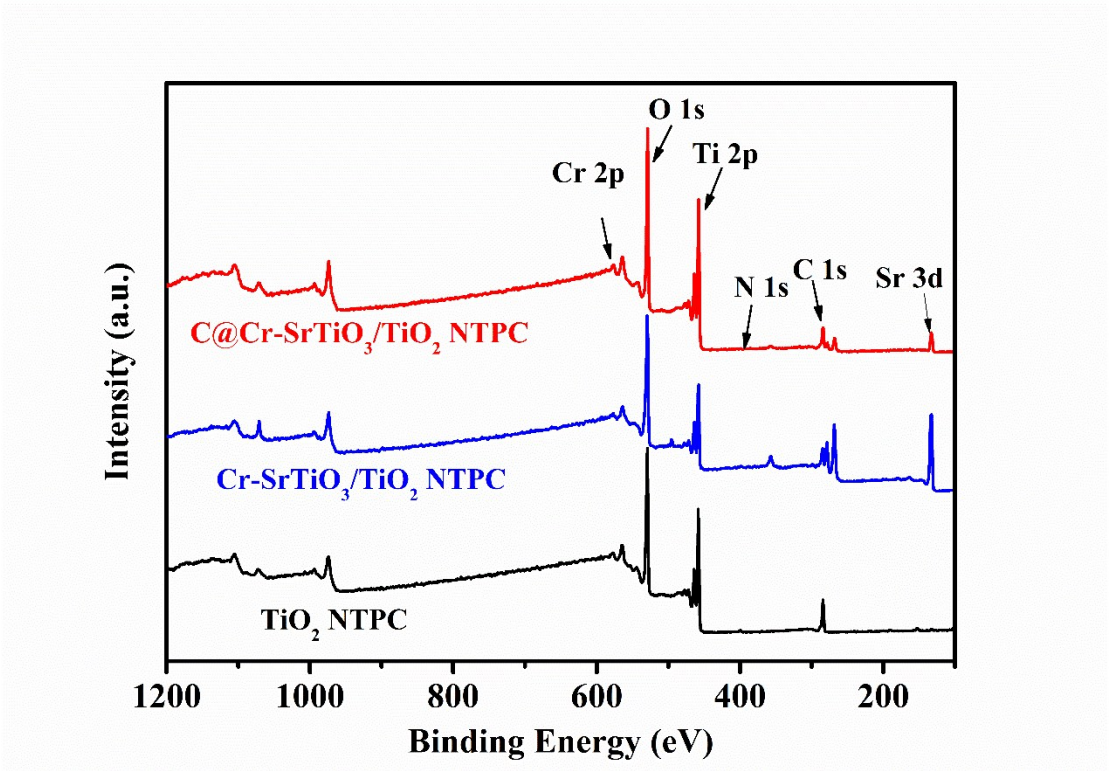

SI-Fig.4 The full scan of different sample photoanodes.

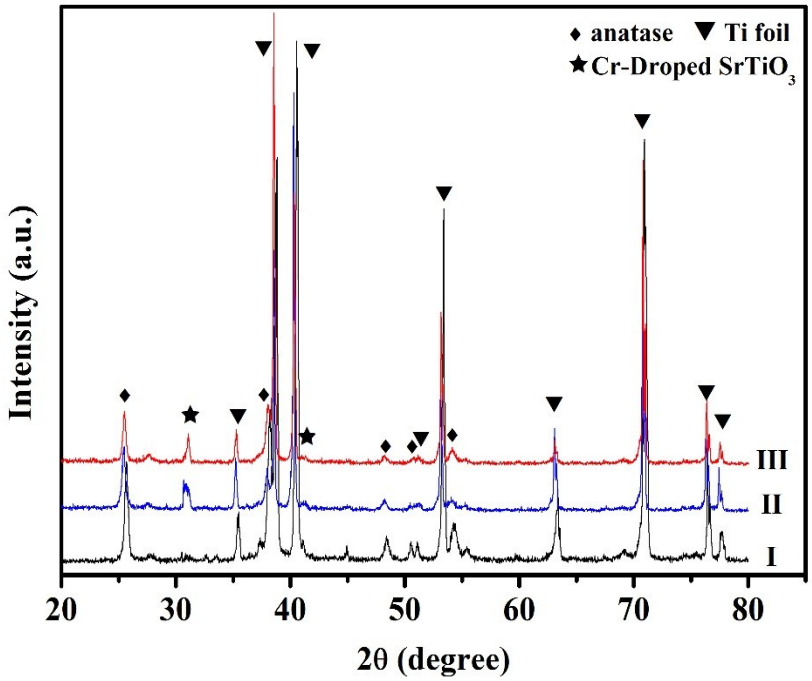

SI-Fig.5 XRD pattern of (I) TiO_2 NTPC, (II)Cr-$SrTiO_3$/TiO_2 NTPC and (III)C@Cr-$SrTiO_3$/TiO_2 NTPC

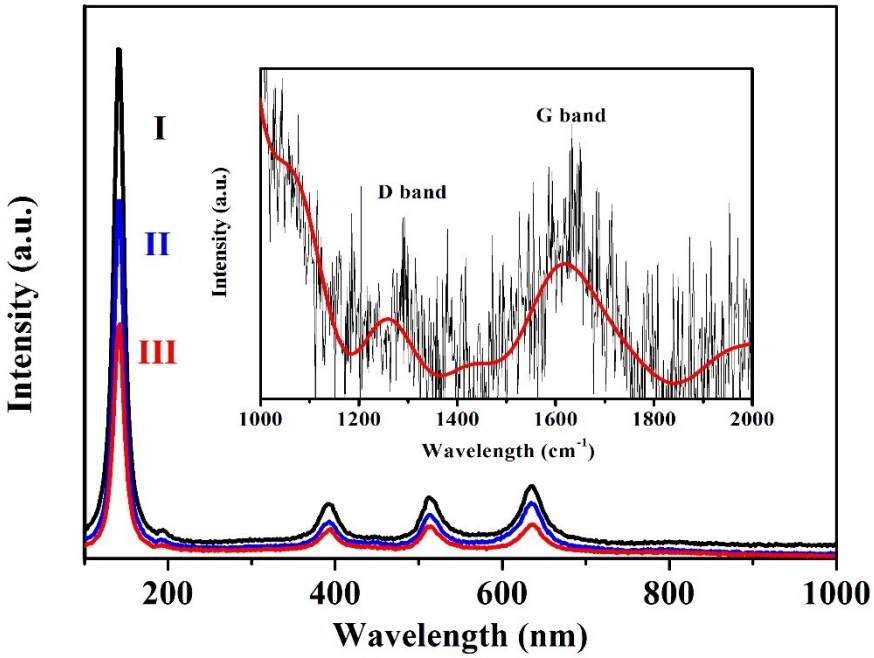

SI-Fig.6 Raman scattering spectra of different sample photoanode.(I: TiO_2 NTPC, II: Cr-$SrTiO_3$/TiO_2 NTPC, III: C@Cr-$SrTiO_3$/TiO_2 NTPC)

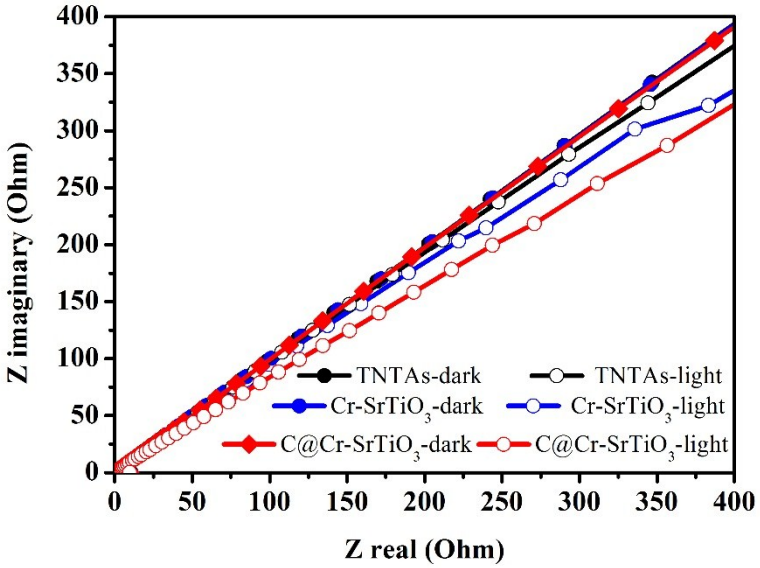

SI-Fig.7 Nyquist plot of as-prepared electrodes

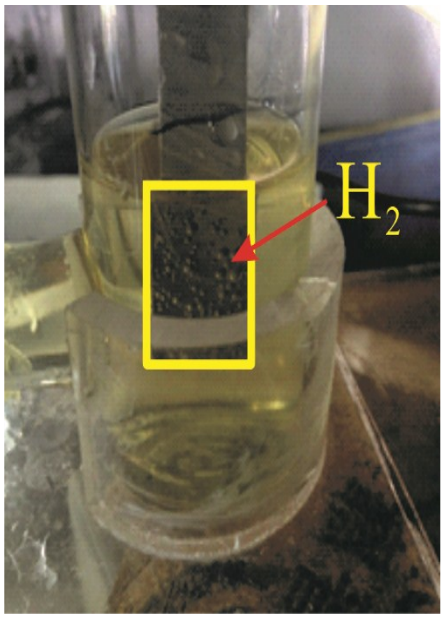

SI-Fig.8 Photoimage of Pt sheet collected at -0.3 V in a 0.5 mol·L^{-1} KOH aqueous solution with 0.1 mol·L^{-1} glucose solution.

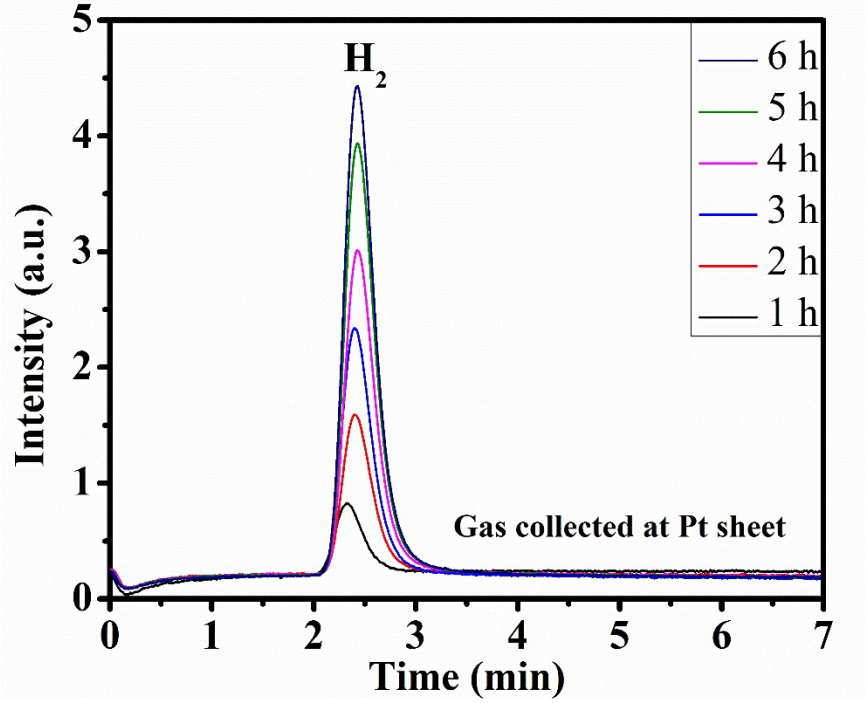

SI-Fig. 9 The chromatogram retention times of the gas collected at Pt sheet at -0.3 V (vs. SCE) under the visible light (100 mW cm^{-2}) irradiation for different reaction time over theC@Cr-$SrTiO_3/TiO_2$ NTPC/Pt system.

SI-Fig.10 Photoimage of photoanode cell for the C@Cr-$SrTiO_3$/TiO_2 NTPC under the visible light irradiation in a 0.5 mol L^{-1} KOH aqueous solution with 0.1 mol L^{-1} glucose solution.